LA-UR 91-3052

LA-UR--91-3052

DE92 000190

Los Alamos National Laboratory is operated by the University of California for the United States Department of Energy under contract W-7405-ENG-36.

TITLE: ATOMIC OXYGEN INTERACTION WITH SPACECRAFT MATERIALS: RELATIONSHIP BETWEEN ORBITAL AND GROUND-BASED TESTING FOR MATERIALS CERTIFICATION

AUTHOR(S): Jon B. Cross, Steven L. Koontz, and Esther H. Lan

SUBMITTED TO: Fifth International Symposium on Materials in Space Environment, 9/16-20/91, Cannes, France

DISCLAIMER

Los Alamos National Laboratory
Los Alamos, New Mexico 87545

FORM NO. 836 R4
ST. NO. 2629 5/81

MASTER

DISTRIBUTION OF THIS DOCUMENT IS UNLIMITED

ATOMIC OXYGEN INTERACTION WITH SPACECRAFT MATERIALS: RELATIONSHIP BETWEEN ORBITAL AND GROUND-BASED TESTING FOR MATERIALS CERTIFICATION

Jon B. CROSS: Los Alamos National Laboratory, Los Alamos, New Mexico 87545
Steven L. KOONTZ: NASA Lyndon B. Johnson Space Center, Houston, Texas 77058
Esther H. LAN: McDonnell Douglas Space Systems Co., Huntington Beach, CA 92647

ABSTRACT

The effects of atomic oxygen on boron nitride (BN), silicon nitride (Si_3N_4), solar cell interconnects used on the Intelsat VI satellite, organic polymers, and MoS_2 and WS_2 dry lubricant have been studied in low Earth orbit (LEO) flight experiments and in our ground-based simulation facility at Los Alamos National Laboratory. Both the in-flight and ground-based experiments employed in situ electrical resistance measurements to detect penetration of atomic oxygen through materials and ESCA analysis to measure chemical composition changes. In the presence of atomic oxygen, silver oxidizes to form silver oxide, which has a much higher electrical resistance than pure silver. Permeation of atomic oxygen through BN overcoated on thin silver (250Å), as indicated by an increase in the electrical resistance of the silver underneath, was observed in both the in-flight and ground-based experiments. In contrast, no permeation of atomic oxygen through Si_3N_4 was observed in either the in-flight or ground-based experiments. The test results on the Intelsat VI satellite interconnects used on its photovoltaic array indicate that more than 60-80% of the original thickness of silver should remain after completion of the proposed Space Shuttle rescue/reboost mission. Gas phase reaction products produced by the interaction of high kinetic energy atomic oxygen (AO) with Kapton were found to be H_2, H_2O, CO, and CO_2 with NO being a possible secondary product. Hydrogen abstraction at high AO kinetic energy is postulated to be the key reaction controlling the erosion rate of Kapton. An Arrhenius-like expression having an activation barrier of 0.4 eV can be fit to the data, which suggests that the rate limiting step in the AO/Kapton reaction mechanism can be overcome by translational energy. Oxidation of MoS_2 and WS_2 dry lubricants in both ground-based and orbital exposures indicated the formation of MoO_3 and WO_3 respectively. A protective oxide layer is formed ≈30 monolayers thick which has a high initial friction coefficient until the layer is worn off. The ground-based results on the materials studied to date show good qualitative correlation with the LEO flight results, thus validating the simulation fidelity of the ground-based facility in terms of reproducing LEO flight results. In addition it has been demonstrated that ground-based simulation is capable of performing more detailed experiments than orbital exposures can presently perform which allows the development of a fundamental understanding of the mechanisms involved in the LEO environment degradation of materials.

INTRODUCTION

The low Earth orbit (LEO) combined environment, consists of ultraviolet and X-ray radiation, charged particles (protons, electrons, and other charged particles), and atomic oxygen all of which can react in a synergistic manner to degrade many commonly used spacecraft materials.[1,2] Because spacecraft travel at 8 km/sec, the surfaces facing the direction of travel (ram direction) experience bombardment by atomic oxygen with a collision energy of ≈5 eV and a flux of $\approx 10^{14}$-10^{15} AO/s-cm^2 or 0.1-1 monolayers/second. Figure 1 depicts the nature and intensity of the various components of the LEO combined natural environment. Since access to LEO is limited and expensive and there is a need for accelerated testing, ground-based testing methodology of materials needs to be developed which takes into account the space combined environment. In order to validate ground-based testing, however, correlation of ground-based data with space flight data is necessary. In this paper, space flight and ground based results for a number of materials

are presented. Materials such as boron nitride (BN) and silicon nitride (Si_3N_4) are of interest to the space materials community because they are candidate optical coatings for spacecraft mirrors; solar cell interconnects lie at the heart of solar power systems; and space qualified lubricants are crucial on long duration missions and must withstand the environment without undergoing significant changes in properties. Boron nitride and silicon nitride coatings were flown in a Space Materials Experiment (SME) sponsored by the Strategic Defense Initiative Organization (SDIO) through the U.S. Army Materials Technology Laboratory (AMTL) and integrated by Sparta, Inc.[3] The SME was a LEO experiment flown as a part of the Delta Star mission, launched March 24, 1989. A variety of materials, including BN and Si_3N_4, were flown on an active panel which was instrumented so that data telemetry to a ground station was possible. In another orbital experiment a set of passive samples of BN, Si_3N_4, silver solar cell interconnects, and dry lubricants were flown on STS-41 and exposed on the STS manipulator arm to ram AO for ≈40 hours for a fluence of $\approx 10^{20}$ AO/cm^2. In addition exposures of these materials were conducted at the Los Alamos National Laboratory simulation (LANL) facility[4] which is capable of exposing materials to hyperthermal atomic oxygen (1-5 eV) over a flux range of 1-10^3 X that of LEO flux as well as VUV radiation at 1236Å. Future work will involve the addition of charged particle beams to the facility in order to fully understand the synergism between the combined environment components.

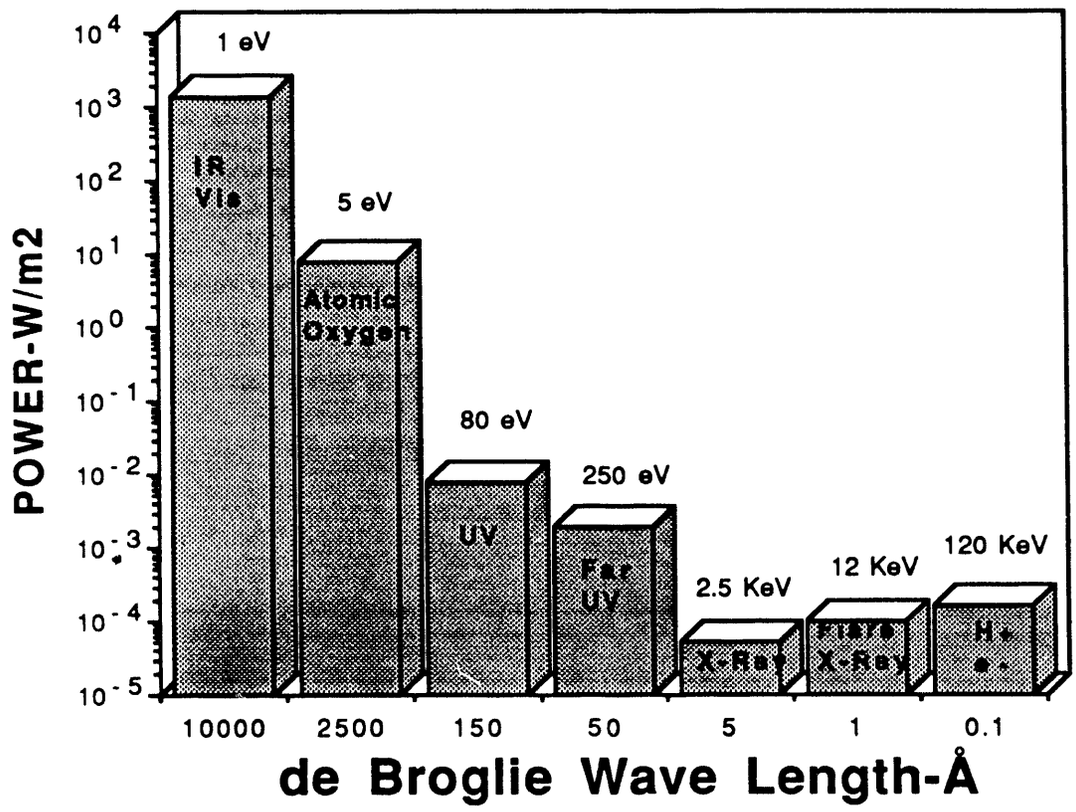

Figure 1. Low Earth Orbit combined natural environment which includes photon radiation, charged particles, and neutral gas species. Energy/particle is also shown.

GROUND-BASED COMBINED EFFECTS TEST FACILITY

The AO source[4] employs a cw plasma produced by focusing a high-power CO_2 laser beam to produce plasma temperatures of 15,000-20,000 K in a rare-gas/oxygen mixture. The high-power cw CO_2 laser (10.6 μm) is used to sustain a spark-initiated plasma in the mixture which subsequently flows through the throat (0.3 mm in diameter) of a hydrodynamic expansion nozzle producing an atomic beam of neutral species. Stagnation pressures of 2-8 atm are used depending on the rare gas; i.e., 2 atm for 50% O_2 in argon and 8 atm for 15% O_2 in helium. A 2.54-cm focal-length ZnSe lens is used to focus the laser beam to a 30-100-μm spot producing power densities of 10^9 W/cm^2, which sustains the plasma at a roughly 50% ionized condition. The lens is moved axially to position the plasma ball in the throat of the water-cooled nozzle. Continuous operation times of greater than 75 hr have been obtained producing fluences $>10^{22}$ O-atoms/cm^2. The source is mounted in a molecular beam apparatus (Fig. 2), where the gas mixture is skimmed after exiting the nozzle and then collimated into a neutral atomic beam of rare gas and O-atoms. The facility consists of 1) the laser-sustained AO beam source, 2) three stages of differential pumping between source and a sample manipulator located 15 cm from the source, 3) a rotatable mass spectrometer with TOF capability for measurements of scattered particle angular and velocity distributions to determine energy accommodation coefficients and gas phase reaction products, and

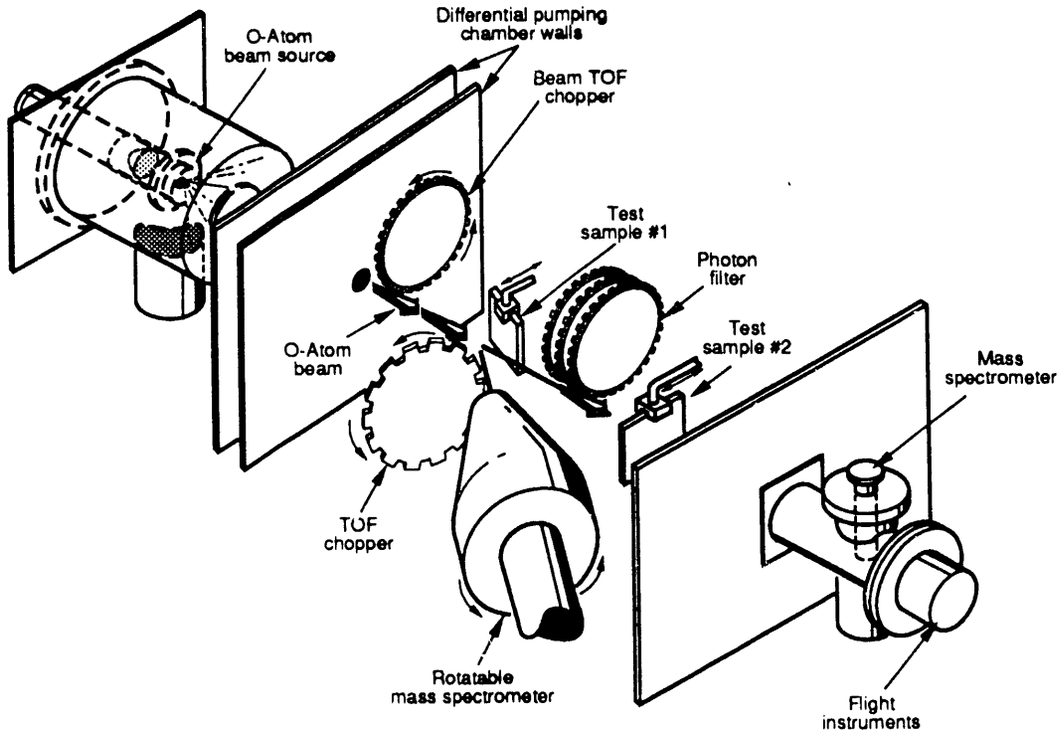

Figure 2. Los Alamos Low Earth Orbit Simulation Facility.

4) a flight mass spectrometer calibration chamber and separate quadrupole mass spectrometer located 120 cm from the source, which is used for beam TOF measurements. At the sample manipulator position, 15 cm from the source, O-atom flux densities of 5 X 10^{16} AO/s-cm^2 are obtained whereas at the flight mass spectrometer position, flux densities of 10^{15} AO/s-cm^2 are recorded. A base pressure of 1 x 10^{-9} Torr is recorded in the sample exposure chamber, which rises to 2 X 10^{-6} Torr when the AO beam is operating. Figure 3 shows an AO energy distributions obtained from time-of-flight (TOF) analysis of the AO beam produced from a plasma of 10%O_2

and 90% Ar. The beam was modulated at 400 Hz and the resulting wave forms for atomic oxygen and the plasma light were recorded with a multichannel scalar. An iterative procedure was implemented to find the velocity distribution,P(v), which when convoluted with the plasma light modulation P(hv) gave the best fit to the atomic oxygen modulation ($F(v)_{exp}$). The convolution was performed using Fourier transform techniques[5] as shown in equation 1

$$F(v)_{exp}=<P'(v)*P'(hv)> \quad (1)$$

where P' denotes the Fourier transform function and <> denotes the Fourier inverse transform. The functional form[6] of P(v) is shown in equation 2

$$P(v)=\text{const.}(v/\alpha_o)^3\exp[-\{v/\alpha_o(1+(\gamma-1)/2M^2)-\gamma^{0.5}M/\sqrt{2}\}] \quad (2)$$

where $\alpha_o=(2kT_o/m)^{0.5}$ at the source temperature T_o, M the local Mach number, γ the ratio of specific heats, m atomic mass, and k the Boltzmann constant. The local beam temperature T is related to M through equation 3. Local Mach numbers of ≈3 were found to fit the experimental

$$T/T_o=[1+(\gamma-1)/2M^2]^{-1} \quad (3)$$

data thus showing the beam to have a local temperature of ≈2000K which is about a factor of two higher than found in low earth orbit. Seeding of oxygen in rare gas mixtures of lower molecular weight than argon lowers the average molecular weight of the mixture and therefore at constant plasma temperature raises the flow velocity out the nozzle and increasing the beam translational energy.

The spectral distribution of the photon component of the atomic oxygen beam was measured using a VUV grating monochrometer which employed photomultiplier detectors having an S-20 response and the other a solar blind photocathode. The spectral distribution of the plasma light source along with the sun distribution are shown in figure 4.

ATOMIC OXYGEN FLUX CALIBRATION

Absolute partial [C_i] number density measurements were made in the chamber used for flight instrument calibration after thermal equilibration of the beam. An orifice of known diameter (1.270 cm) operating under effusive flow conditions was employed to pump on the chamber having a known temperature T(ch). The beam fractional (f_i) composition was measured using lock-in detection of the modulated beam and a residual gas analyzer corrected for known relative ionization cross sections while the total absolute number density (C_o) was measured using a spinning rotor gauge. From these data, the partial flux density (F_i) of each component of the beam was

$$F_i=1/4[C_i]<V_i> \quad (4)$$

determined from equation 4 where $<V_i> = [8kT(ch)/\pi m_i]^{1/2}$ is the average thermal accommodated velocity, k is the Boltzmann constant, m_i is the atomic mass of the ith species, and $[C_i]=f_i*C_o$. This technique produces AO flux values having a run-to-run variation of 20%. The fractional dissociation of the beam between AO and O_2 depends upon the source pressure, fraction of O_2 in the O_2/rare gas mixture, and position of the plasma ball in the nozzle but runs between 60-90%.

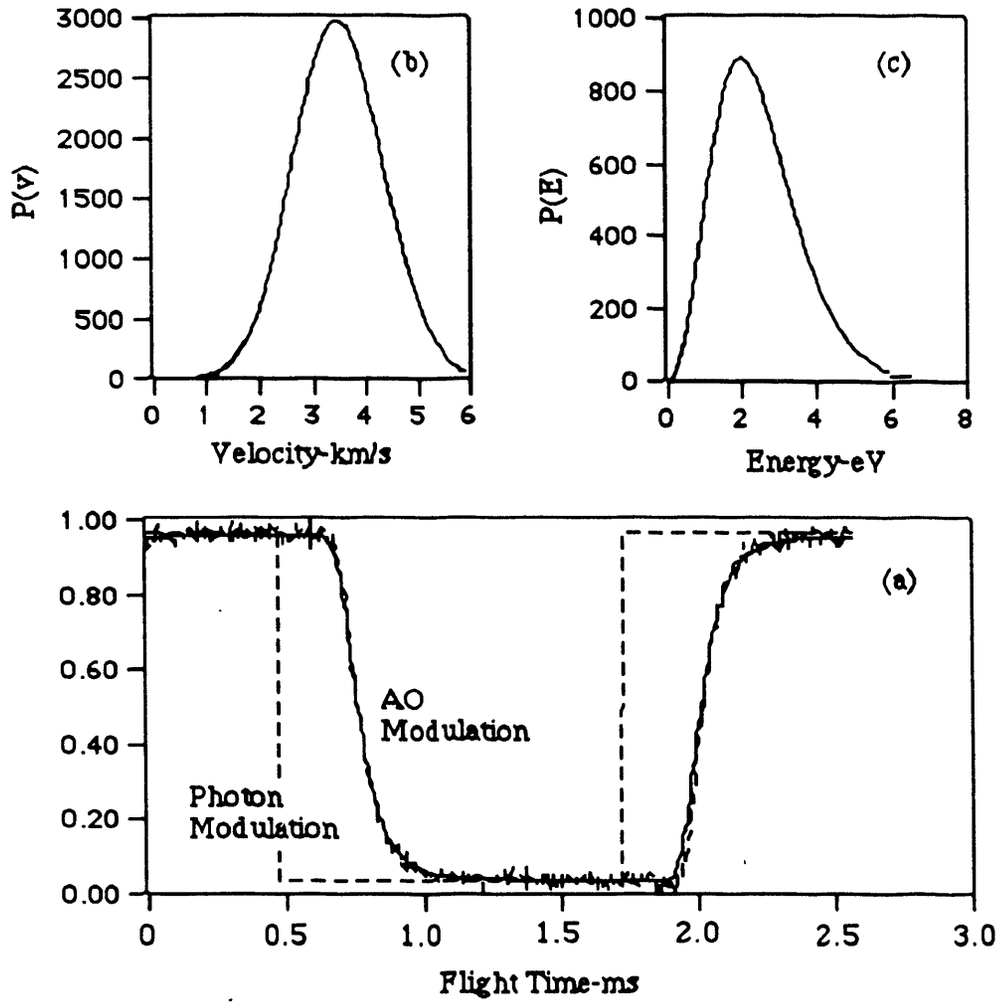

Figure 3. Modulated direct atomic oxygen beam (····) and plasma light (----) signals (a) with resulting fit (—)produced by velocity distribution (b) having an energy distribution (c).

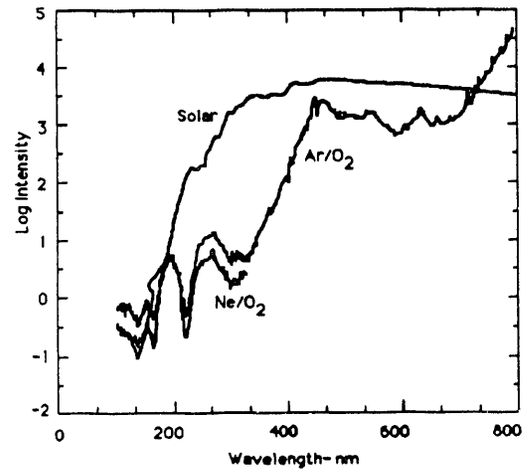

Figure 4. Spectral distribution of atomic oxygen plasma source and solar spectrum (W/m^2) is shown for reference.

THIN FILM OPTICAL QUALITY COATINGS

Techniques and Experimental Conditions

The technique used to evaluate the BN and Si_3N_4 films in both the Delta Star and STS-41 space flight and LANL ground-based experiments consists of using silver oxidation as a sensor for atomic oxygen penetration through the films.[7] The sensor has two strips of silver (≈250Å) deposited on top of an alumina or sapphire substrate (Figure 5). Coatings of known thickness are deposited over the silver films, and the electrical resistance of the silver is measured in situ during exposure to detect atomic oxygen penetration through the coating. Silver oxidizes in the presence of atomic oxygen with near 100% efficiency to form silver oxide, and the electrical resistance of the oxide is much higher than that of pure silver. The electrical resistance data for silver is converted to electrical conductance (inverse of electrical resistance) to evaluate the thickness of silver remaining since electrical conductance is proportional to the thickness of a conductor.

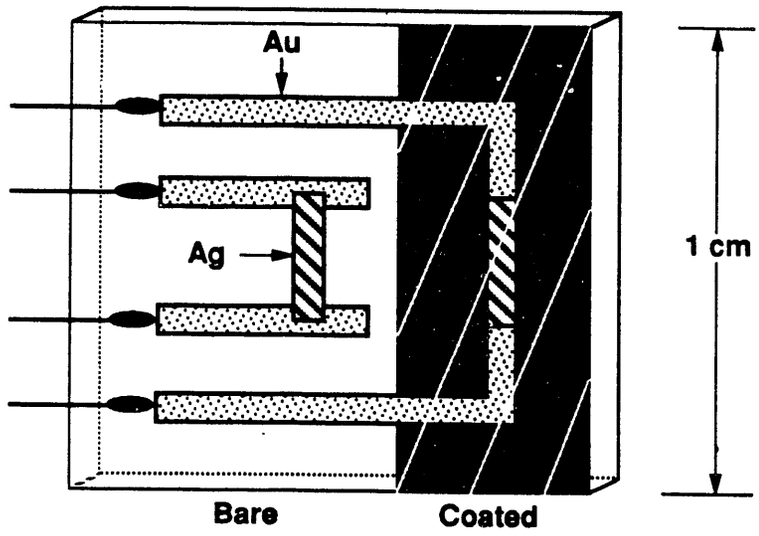

Figure 5. Atomic oxygen sensor. Thick (10-20 microns) gold lead-in wires are deposited on insulating substrate. Thin (250Å) silver film is deposited and overcoated with film of interest.

The Delta Star SME spacecraft was flown in LEO at an altitude of 500 km and inclination of -48° with an estimated flux of 1.8×10^{13} atoms/cm^2-sec for approximately nine months with active data acquisition. While in orbit estimated sample temperatures varied between 10°C and 40°C. The STS-41 exposure was performed on the STS manipulator arm at a flux level of $\approx 7 \times 10^{14}$ atoms/s-cm^2 and a substrate temperature ranging between -10 to 50°C for a 40-hour time period (fluence $\approx 10^{20}$ atoms/cm^2). Ground-based LEO simulation facility exposures were performed at atomic oxygen kinetic energy of 2 eV and flux of 4.5×10^{16} atoms/cm^2-sec.

Results

Permeation of atomic oxygen through Si_3N_4 was not observed in either the space flight results (Delta Star and STS 41) or the ground based results. The Delta Star flight and ground-based (GB) results are presented in Figure 6 which shows the conductance of silver beneath the Si_3N_4 films plotted as a function of atomic oxygen fluence.

Auger analysis of a sample with 700Å Si_3N_4 coated over Ag (≈250Å) on a Si wafer substrate showed that after atomic oxygen exposure at LANL (2.2 eV, 210°C, total fluence of 4.7×10^{20} atoms/cm^2), the oxygen concentration at the surface increased from 23 atomic % to 42 atomic %,

while the nitrogen concentration at the surface decreased from 24 atomic % to 12 atomic %. Auger depth profile of the exposed sample indicated that oxygen was present only within 50Å of the surface. Optical microscopy up to 100X magnification and SEM up to 10,000X magnification of Si_3N_4 coated oxygen sensors did not reveal microcracking of the Si_3N_4 films after exposure at LANL. TEM was used to study Si_3N_4 films which had been deposited on sodium chloride (NaCl) crystals before and after ground-based atomic oxygen exposure. The films showed some microcracking which appeared to be primarily in areas where there were irregularities on the NaCl surface. Electron diffraction was also performed on the Si_3N_4 films and indicated that the film was amorphous before and after atomic oxygen exposure.

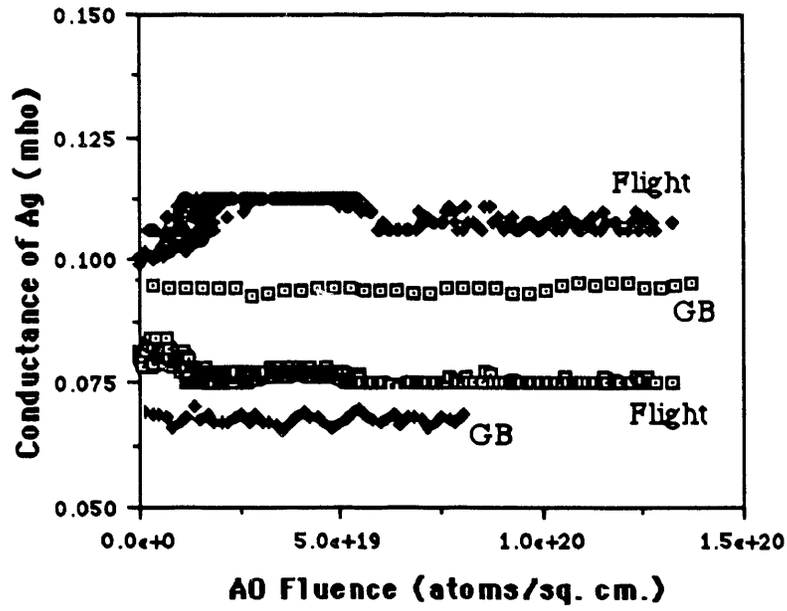

Figure 6. Panel shows Delta Star SME flight results for two Si_3N_4 films 0.7μm (star) and 0.35μm (square) thick on a rough alumina substrate. GB (ground-based) shows laboratory results for a 700 Å thick Si_3N_4 film on a smooth sapphire substrate.

Permeation of atomic oxygen through BN was observed in both space flights (Delta Star and STS-41) and the ground-based results. Figure 7 shows the Delta Star flight data, the ground test results, and the STS-41 results. All boron nitride samples show the conductance steadily decreasing when exposed to increasing atomic oxygen fluence. Auger depth profiles of 750Å BN coating over Ag (≈250Å) on a Si wafer substrate exposed in the ground based facility showed oxygen and carbon, in addition to boron and nitrogen, through the entire thickness of samples both before and after atomic oxygen exposure (2 eV, 45°C, total fluence of 1.7×10^{20} atoms/cm^2-sec). The carbon concentration in both the exposed and unexposed samples was estimated to vary between 5 and 15 atomic % through the thickness of the films. The oxygen concentration in both the exposed and unexposed samples was estimated to vary between 5 and 20 atomic % through the thickness of the films. A 25% decrease in the thickness of the BN film after exposure at LANL was detected in the Auger depth profile and confirmed using ellipsometry. Optical microscopy up to 100X magnification and SEM up to 10,000X magnification of BN coated sensors after exposure at LANL did not reveal microcracking in the film. In contrast to the ground-based results, data on BN from the Delta Star SME did not indicate erosion of this material during exposure to the LEO environment. A BN (0.1 μm) coated quartz crystal microbalance (QCM) was included in the SME, and results showed a slight mass gain of 0.75 μg/cm^2 rather than loss after 150 days of

mission elapsed time. It is unclear at this time whether the mass gain was due to contamination of the surface or due to oxygen incorporation into the BN.

Discussion

Ground-based facility results shows good agreement with space flight data for both Si_3N_4 and BN. Atomic oxygen removes nitrogen from Si_3N_4 through ,most likely, the formation of nitrogen oxides (NO,NO_2) which are volatile and then forms SiO_2 which has a very low diffusion rate for AO and protects the underlying nitride from further reaction. The conversion of Si_3N_4 to SiO_2 has been observed in both thermal atomic oxygen[8] and hyperthermal atomic oxygen reactions.[9]

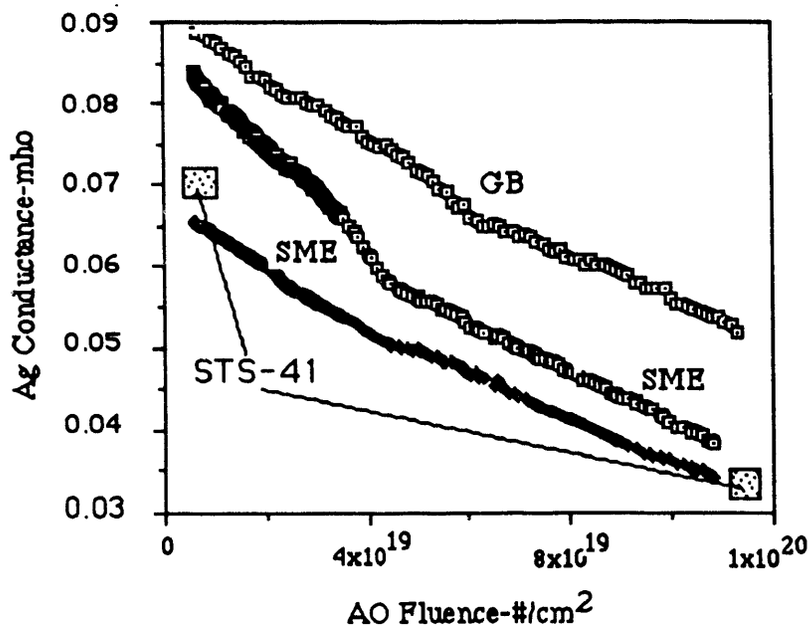

Figure 7. Plot shows Delta Star SME flight results using 1 μm thick BN films over 250Å Ag film on rough alumina substrates and STS 41 flight and laboratory results (GB) for 750Å thick BN films on smooth sapphire substrates. Decreasing conductance of silver film indicates that atomic oxygen is penetrating the film.

The space flight and ground based data for BN showed that there was oxygen transport through this material resulting in oxidation of silver underneath the BN. Direct correlation of the rate of oxygen transport through the BN (rate of oxidation of the silver) from the space flight (SME) and ground based data was not attempted because of the differences in the preparation techniques and thickness of the BN films as well as the differences in the substrate surface roughness on the sensors. Even though the ground based results showed a thickness loss in the BN, the remaining thickness of this material during atomic oxygen exposure was sufficient to cover completely the silver surface. There was oxidation of silver underneath, and therefore, oxygen transport through the remaining BN overlayer. The BN thickness decrease found in the laboratory exposure results is attributed to hydrated boron oxide leaching caused by water attack on the boron oxides[10] when the sample was exposed to laboratory air environment during sample transfer to the surface analysis apparatus. Immediately after removing the BN AO exposed sample from the ground-based facility a well defined AO beam image was observed which subsequently disappeared after a one week exposure to laboratory air during shipment from Los Alamos to McDonnell Douglas Corporation. The SME flight experiment BN coated QCM however showed a small mass g. rather than loss since water is not present in LEO to form the volatile hydrated

boron oxides and therefore oxygen would remain incorporated in the film. Ground-based QCM mass change measurements are planned in the future to confirm this hypothesis.

A more detailed study than the one presented here is needed before definite conclusions can be drawn on the effect of translational energy. However there exist calculations[11] which indicated that surface barriers larger than the bulk diffusion barriers can exist for certain materials which would imply that translational energy may be effective in surmounting the surface barrier which would be the rate limiting step in oxygen permeation. The magnitude to these surface barriers are related to the elastic constants of the material in question, i., e., soft materials, which BN is, have in general lower barriers to oxygen penetration than hard materials such as SiO_2. A general conclusion that can be drawn from these reports and our results is that soft optical coatings should be avoided or at least be thoroughly investigated if long term exposure to the LEO environment is contiplated.

INTELSAT-VI SOLAR ARRAY INTERCONNECTS

A Hughes 506-type communications satellite belonging to the Intelsat organization was marooned in low Earth orbit on March 14, 1990, following failure of the Titan third stage to separate properly. The satellite, Intelsat VI, was designed for service in geosynchronous orbit and contains several material configurations which are susceptible to attack by atomic oxygen. Analysis showed the silver foil interconnects in the satellite photovoltaic array to be the key materials issue because the silver is exposed directly to the atomic oxygen ram flux. Laboratory testing became vital on finding that values of the reactivity of silver with atomic oxygen reported in the literature ranged over nearly two orders of magnitude and that the total number of published measurements is relatively small.

Ground-based[12] and flight tests[13] were conducted on samples of silver interconnect material from the same production lot used to build the Intelsat VI solar arrays. In addition, ground-based and flight configuration tests were conducted on a solar cell test article cut from a ground test solar array which is essentially identical to the Intelsat VI solar array. Atomic oxygen degradation of the interconnect silver was determined by: 1) mass loss after removing silver oxide by dissolving with ammonium hydroxide, 2) scanning electron microscopy (SEM) thickness measurements after removal of silver oxide, 3) real time electrical conductivity measurements (during oxygen atom exposure), 4) optical microscopy, and 5) real time solar cell performance (during oxygen atom exposure and thermal cycling). The specimens were exposed to total atom fluences comparable the the expected fluence for the Intelsat VI vehicle; on the order of $5x10^{20}$ AO/cm^2. The test specimens in the ground-based facility were held at various temperatures and, in some instances, subjected to thermal cycling during atom exposure to produce data which describes the temperature dependence of the degradation reaction and the effects, if any, of thermal cycling.

The thickness of the oxide layer formed and it's effect on the degradation kinetics depends strongly on the temperature of the silver interconnect. The ground-based results showed no spontaneous spalling or flaking of the silver oxide layer at any temperature, though thick oxide layers which formed on the solar cell test article interconnects did flake off to a limited extent during shipment from Los Alamos to Johnson Space Center. Interconnect thickness loss was less than 5 % for interconnect temperatures below 80°C and oxygen atom fluences of up to $2x10^{20}$ atoms/cm^2. Even lower thickness loss was calculated from changes in interconnect electrical conductance measured during oxygen atom exposure, suggesting that a conducting or semiconducting oxide forms on silver surfaces exposed to high velocity oxygen atoms. There were no detectable changes in interconnect electrical conductance with samples temperatures of 20 or 40°C and comparable oxygen atom fluences. Weight gain/loss measurements allowed calculation of the stoichiometry of the silver oxide films, i.e., weight gain was detected after AO exposure but before ammonium hydroxide dissolving of the silver oxide. The 75 °C interconnect specimen produced an $Ag_{1.78}O$ film while the 150°C specimen produced an $Ag_{1.85}O$ film. The oxides are oxygen rich indicating a mixture of Ag_2O and AgO.

Both high and low temperature interconnect specimens showed logarithmic rates of conductance loss while in the ground-based oxygen atom beam, a result consistent with slow diffusion of reactive species through a surface oxide barrier. An activation energy of of 10-20 kcal/mole was calculated from the temperature dependence of oxide film growth kinetics in the logarithmic domain. At 150°C, shown in Figure 8, a specimen displayed a change from logarithmic to linear oxidation kinetics for oxygen atom fluences greater than 10^{20}. The change from logarithmic to linear oxidation kinetics most likely indicates the development of cracks or pores in the surface oxide barrier layer. The 150°C interconnect specimens showed a 30% thickness loss by SEM at a fluence of $2x10^{20}$ oxygen atoms (logarithmic kinetics) and a 67% decrease in silver thickness by mass loss at a fluence of $5.5x10^{20}$ AO/cm^2 (log kinetics to $1.5x10^{20}$ AO/cm^2 then linear kinetics to $5.5x10^{20}$ AO/cm^2).

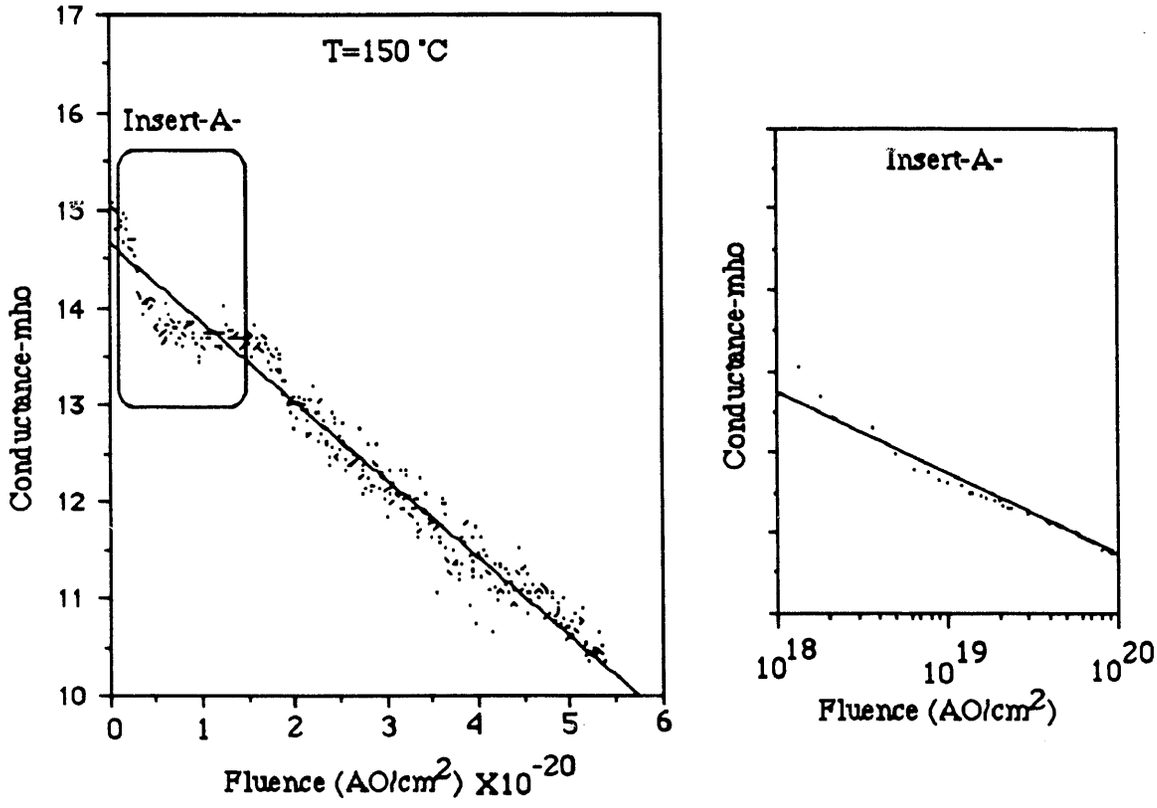

Figure 8. Electrical conductivity of Intelsat VI silver interconnect foil at T=150°C. Note logarithmic relationship between conductance and O-atom fluence shown in insert -A- and a subsequent change to a linear relationship which is attributed to crack formation in the silver oxide corrosion product.

The solar cell test article (STA) was exposed to 10^{20} AO/ cm^2 at a cell surface temperature of 50°C, and then $2.5x10^{20}$ AO/cm^2 while the STA was thermal/photo cycled between 30 and 130°C 68 times. The same solar simulator lamp used to produce thermal cycling also produced photocurrent in the exposed cell interconnects, resulting in a more realistic reproduction of on orbit operation. Despite thermal cycling at much higher temperatures than are expected for the Intelsat VI itself, no degradation of cell output (Figure 9) was observed after a total oxygen atom fluence of $\approx 3x10^{20}$ AO/cm^2.

An orbital test called INTELSAT SOLAR ARRAY COUPON (ISAC)[13] was flown in October 1990 on STS-41. It consisted of two witness plates with samples of silver interconnects and operational solar cell panels mounted on them. Analysis of the returned silver interconnect specimens indicate an erosion rate of 1.04 $\mu m/10^{20}$ AO/cm^2 which at the time of reboost in April 1992 represents a 36% loss of silver to silver oxide. The both sides of the interconnect material were oxidized and blistered and there was no evidence that the oxide layer had sloughed off. The two solar cell panels showed no degradation of electrical power output. The ground-based and orbital exposure results show qualitative similar results with the bottom line being that the satellite's solar cell output will not be adversely affected by its sojourn in low earth orbit.

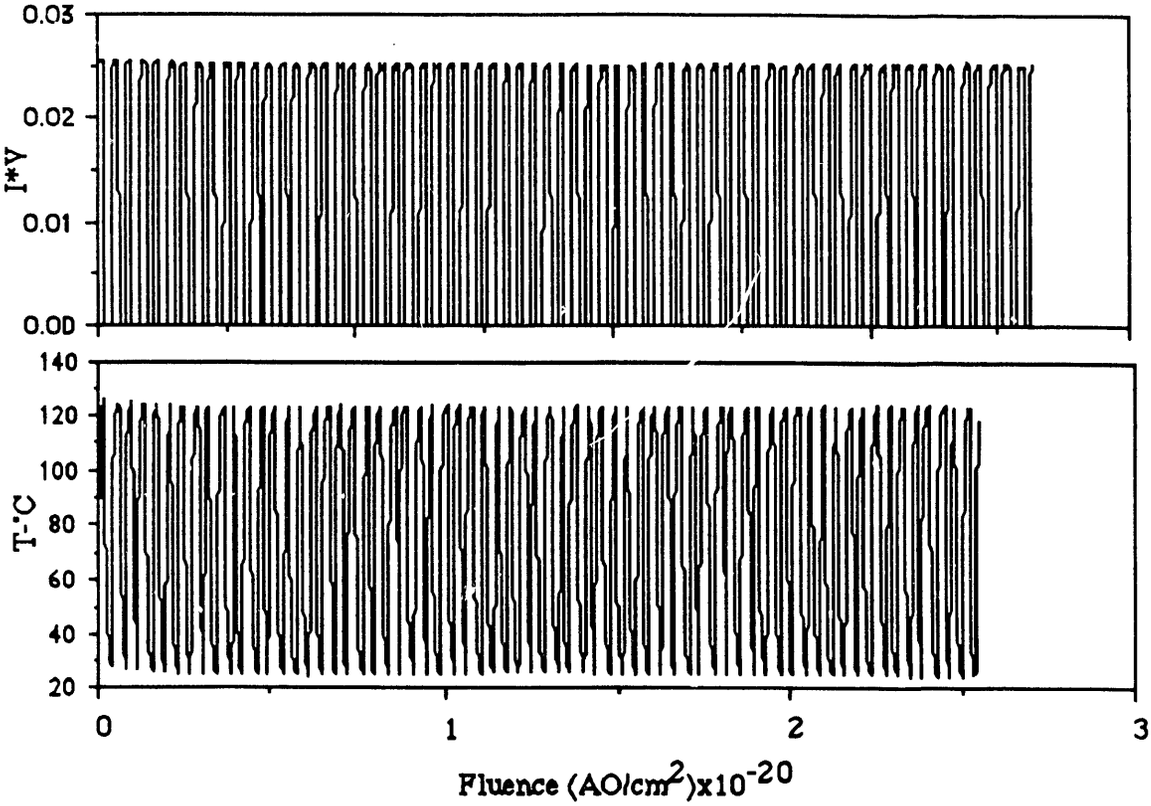

Figure 9. Solar cell test article power output and temperature during thermal cycling and simultaneous atomic oxygen exposure in the AO ground-based LEO simulator.

ORGANIC POLYMER DEGRADATION

The reactivity of Kapton with atomic oxygen under various exposure conditions is plotted versus relative translational energy in Figure 10. Estimates of reactivity in a O_2/F_2 plasma reactor[14]have been included to emphasize the primary conclusion that translational energy plays a key role in polymer degradation in low earth orbit. At high collision energy approximately 10% of the AO reacts to form volatile products while the remaining 90% desorps from the surface with a translational temperature roughly equal to the polymer surface temperature. An Arrhenius-like expression having an activation barrier of 0.4 eV can be fit to the data[15] suggesting that a rate limiting step exists in the AO/Kapton reaction mechanism which can be overcome by translational energy. A number of other types of polymers also have reactivities with hyperthermal AO similar to that of Kapton[1], suggesting that not only is a translational barrier dominating the overall reaction mechanism of hydrogen terminated polymers but that structural differences between the polymers

are unimportant. This conclusion is also substantiated by oxygen-based resist stripping studies, which have found that substitution of halogen atoms for AO greatly increases thermal reaction rates due to the lower activation energy for hydrogen abstraction by halogens[16]. A question still remains concerning the details of the reaction anisotropy ; i.e., whether there is a continual direct attack by hyperthermal AO on the polymer backbone producing chain scission or whether thermalized surface adsorbed free radicals produce the chain scission (reactions 2B and 7) as is

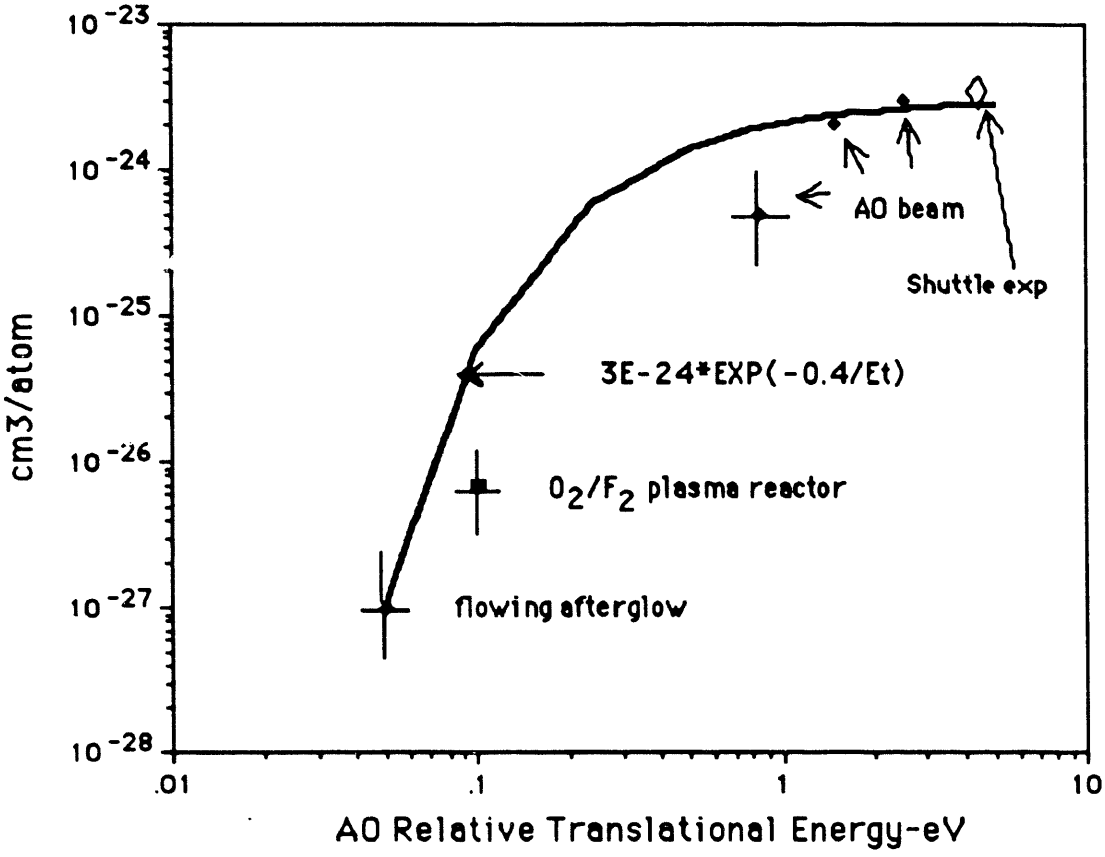

Figure 10. Reactivity of Kapton as a function of atomic oxygen translational energy. Note that an Arrhenius-like expression having an activation barrier of 0.4 eV can be fit to the data.

Insertion	RH + O	⇒	RO· + H (E_a≈0.1 eV)	(1A)
Abstraction	RH + O	⇒	R· + OH (E_a≈0.4 eV)	(1B)
	R· + O	⇒	RO·	(2A)
	R· + O	⇒	RO* (internal excitation)	(2B)
	RO· + O	⇒	RO2·	(2C)
	R· + O2	⇒	RO2·	(3)
	RH + OH	⇒	R· + H2O	(4)
	ROO· + R'H	⇒	ROOH* + R'·	(5)
	ROOH*	⇒	RO· + OH	(6)
	RO*	⇒	chain scission	(7)

Table 1. Proposed reaction mechanism for hyperthermal atomic oxygen degradation of hydrogen terminated polymers.

shown in the proposed mechanism in Table 1. The reaction efficiency curve in Figure 10 should continue to increase to values greater than 10% if the conjugated C=C polymer backbone scission were sensitive to AO translational energy. As that is not the case, i.e., the efficiency levels out to 10-20% at energies above 1 eV, there must be another rate-limiting step in the degradation that caps the reaction efficiency at about 10% independent of the AO translational energy. One possible candidate is reaction 2B, where the extent of internal excitation of RO*· is determined by the RO* molecular structure while increasing the AO translational energy only changes the concentration of RO*.

It is evident from these results that conclusions deduced from experiments employing thermalized AO (ashers, flowing afterglows, etc.) must be very carefully considered before applying them to low earth orbit phenomena. The available data show that the common practice of reporting "equivalent on orbit oxygen fluence" based on the mass loss rate of Kapton in an asher or flowing afterglow has no basis in physical fact and can be dangerously misleading[17].

WS_2 and MoS_2 DRY LUBRICANTS

In two previous studies[18,19] the oxidation properties of various crystalline forms of MoS_2 were investigated under conditions that simulate the LEO environment in order to determine possible tribological implications for lubricating films used on spacecraft. A number of conclusions were drawn from that work: 1) exposure of MoS_2 to energetic atomic oxygen under anhydrous conditions resulted in the formation of predominantly MoO_3 in the near-surface region with lesser amounts of MoO_2; 2) the oxide layer is roughly 10-30 monolayers thick; 3) the extent of oxidation is essentially independent of crystallographic orientation of the MoS_2; 4) diffusion of oxygen atoms through the oxide layer is very slow; 5) the reactivity of MoS_2 to hyperthermal atomic oxygen is initially 50% that of AO toward Kapton; 6) that thermal atomic oxygen has almost the same reactivity to MoS_2 as hyperthermal atomic oxygen; 7) sulfate's were found to form when there was water present (OH) in the exposure system; 8) initial friction of the film was high (0.25) and dropped to a low value after breaking through the oxide film. It was concluded that a continuous flux of atomic oxygen striking a MoS_2 surface would result in a high average friction coefficient which would depend upon the speed per cycle and absolute value of the O-atom flux.

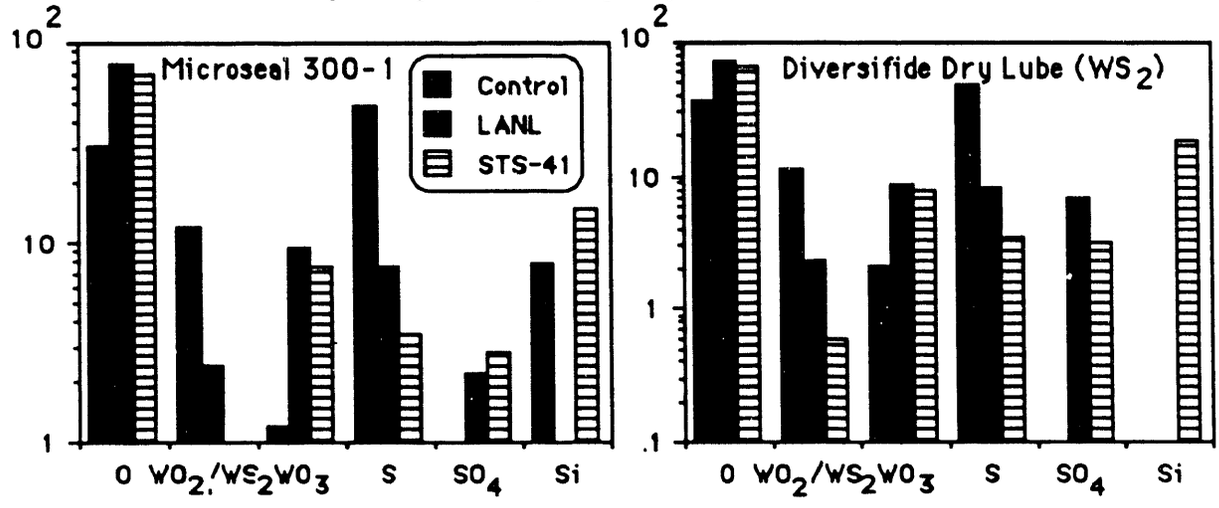

Figure 11. X-Ray Photoelectron Spectra (XPS) of WS_2 lubricants exposed to simulated and actual LEO environments. Intensities are in atom percent.

At the time of these lubricant studies there were no orbital exposure results with which to compare. Lubricant samples were subsequently flown on STS-41 in conjunction with the Intelsat VI silver interconnect study and ground-based exposures were performed on identical samples of

dry lubricants. Figure 11 shows the XPS analysis results of exposing WS_2 to both the LEO and simulated LEO environments. Intensities are in atom percent with an unexposed control, LANL ground-based and STS-41 orbital exposure results being shown. Note that for both ground-based and orbital exposures, 1) the oxygen content increases, 2) the intensity of WS_2/WO_2 decreases, 3) WO_3 increases, 4) sulphur decreases, 5) sulfate's are present. Note also that a silicon contaminant is present in the orbital exposures and on one control sample and that there is some oxygen in the original samples due to their manufacturing processing. Friction and wear testing have not been performed as these samples were not configured for these tests.

Figure 12 shows XPS analysis of MoS_2 Everlube 1346 which contains polydimethyl siloxane binder and MoS_2 Premaslick R which contains polyurathane binder. Note that the Everlube 1346

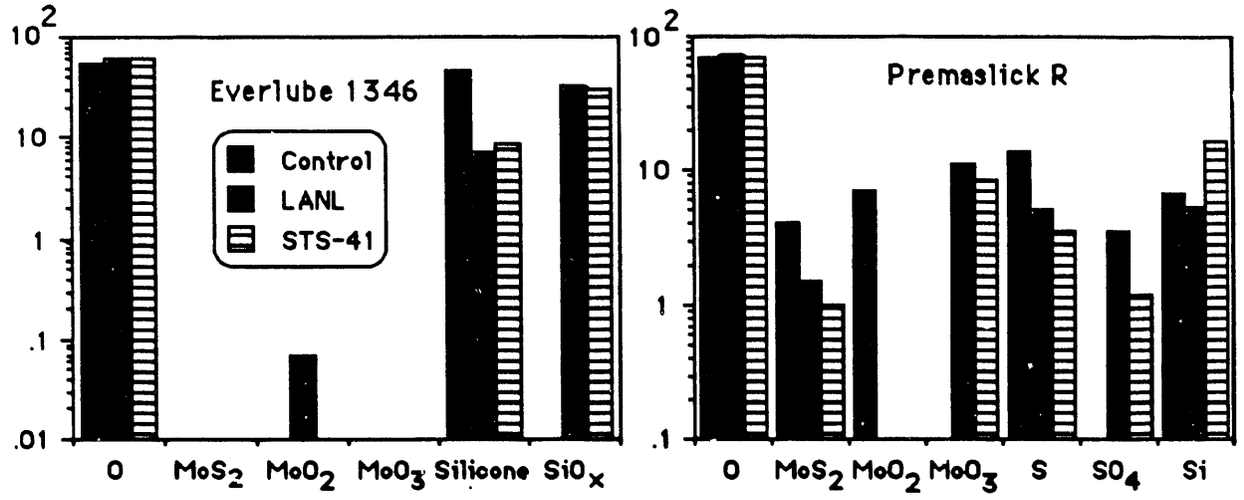

Figure 12. XPS spectra of MoS_2 dry lubricants. Everlube 1346 contains a polydimethyl siloxane binder and Premaslick R contains a polyurathane binder. Intensities are in atom percent.

shows in both the ground-based and orbital exposures no indication of MoS_2 and shows chemical alteration of silicone to SiO_2. The Premaslick R with the polyurathane binder on the other hand shows marked changes similar to the WS_2 results. Note the burn-out of sulphur and the complete oxidation of MoO_2 to MoO_3. These results are in good agreement with the results of the previous laboratory studies[18,19] of MoS_2 including the presence of SO_4 and therefore indicate that protection of dry lubricants will be needed when they are operated under high fluence atomic oxygen conditions.

CONCLUSION

The examples shown in this paper indicate that the cw atomic oxygen beam source described here reproduces qualitatively the orbital exposure results. Thin films have been shown to be resistant to atomic oxygen attack if they are hard and that soft (low shear strength) films are susceptible to AO attack. Solar cell interconnects made of thin silver ribbon have been shown to form a protective silver oxide overlayer which does not slough off, thus protecting the underlying silver and that there is no degradation of the solar cell power output during thermal cycling and simultaneous AO exposure. It has been shown that hydrogen terminated polymers, i.e., nonfluorinated polymers, have a reaction efficiency which is strongly dependant upon the atomic oxygen translational energy and that the use of Kapton as a fluence detector in thermal atomic oxygen sources such as plasma ashers is inappropriate. Very few of the process underlying atomic oxygen degradation of spacecraft materials have a sharp energy thresholds such as would be expected for collisional ionization, therefore the differences that exist between the simulated and actual LEO environments do not make large differences in the exposure results. The important point to remember is that a fundamental understanding of the interaction mechanisms is needed to

interpret the results of ground-based and LEO exposures. For example, even though Kapton was exposed at a nominal collision energy of 2 eV with a 1-2 eV spread in energy while the orbital exposures were performed at ≈5 eV with a spread in energy ≈1/2 that of the ground-based source, the results can be correlated because the underlying chemical mechanism is understood, i.e., the data are correlated through an Arrhenius expression involving kinetic energy not substrate temperature. It is evident from these results that orbital exposure results alone are not sufficient to fully characterize the interaction of the LEO environment with materials. LEO exposure experiments are needed to validate ground-based results but only through the use of ground-based LEO simulation facilities can complete evaluation and characterization of materials before, during and after exposure be obtained, mechanisms deduces, and accelerated testing be performed. With a fundamental understanding of the mechanisms of LEO environmental effects on material, full-life material certification tests can then be confidently undertaken in ground-based simulation facilities at a small fraction of the cost of orbital exposures.

ACKNOWLEDGEMENTS

The authors wish to thank SDIO and AMTL for the use of the data from the Delta Star Space Materials Experiment. We also thank Lubert Leger of NASA/JSC for many helpful discussions and support of the LANL facility. The invaluable technical assistance of Frank Archuleta (LANL) is gratefully acknowledged.

References

1. J. T. Visentine, L. J. Leger, J. F. Kuminecz, and I. K. Spiker, "STS-8 Atomic Oxygen Effects Experiment," AIAA paper 85-0415, Proceedings from the AIAA 23rd Aerospace Sciences Meeting, January 1985.
2. W. S. Slemp, B. Santos-Mason, G. F. Sykes, and W. G. Witte, "Effects of STS-8 Atomic Oxygen Exposure on Composites, Polymeric Films, and Coatings," AIAA paper 85-0421, Proceedings from the AIAA 23rd Aerospace Sciences Meeting, January 1985.
3. S. Rosenwasser, "Delta Star Space Materials Experiment Data Analysis," 7th US/UK SDI Key Technologies SCORE Group Meeting, June 1990.
4. J. B. Cross and N. C. Blais, "High-Energy/Intensity CW Atomic Oxygen Beam Source" Progress in Astronautics and Aeronautics, Vol. 116, 1989.
5. J.A. Serri, M.J. Cardillo, and G.E. Becker, "A Molecular Beam Study of the NO Interaction with Pt(111)", J.Chem. Phys., 77, 1982.
6. H. Pauly and J.P. Toennies, "Beam Experiments at Thermal Energies", Methods of Experimental Physics, Vol. 7-Part A, 1968, Academic Press, New York & London.
7. J. B. Cross, E. H. Lan, C. A. Smith, and R. M. Arrowood, "Evaluation of Atomic Oxygen Interaction with Thin-Film Aluminum Oxide," Proceedings from the 3rd International Conference on Surface Modification Technologies, August 1989.
8. D. A. Gulino, R. A. Egger, and W. F. Banholzer, "Oxidation-Resistant Reflective Surfaces for Solar Dynamic Power Generation in Near Earth Orbit," J. Vac. Sci. Technol. A, vol. 5, no. 4, Jul/Aug.1989, pp. 2737-2741.
9. J. C. Gregory, M. J. Edgell, J. B. Cross, and S. L. Koontz, "The Growth of Oxide Films on Metals under the Influence of Hyperthermal Atomic Oxygen," 119th TMS Annual Meeting and Exhibit, February 1990.
10. Kirk-Othmer Encyclopedia of Chemical Technology, 3rd ed., vol. 4, 1978, pp. 68-70.
11. M. Ronay and P. Nordlander, Phys. Rev. B, 35, 9403 (1987).
12 S.L. Koontz, J.B. Cross, M.A. Hoffbauer, and T.D. Kirkendahl, "Atomic Oxygen Degradation of Intelsat VI-Type Solar Array Interconnects: Laboratory Investigations", NASA Technical Memorandum 102175, March, 1991.
13. A. Dunnet and T.D. Kirkendall, "Assessment of Atomic Oxygen Erosion of Silver Interconnects on Intelsat VI.F3", private communication.
14. M.A. Hartney, D.W. Hess, and D.S. Soane, J. Vac. Sci. Technol., B7(1), 1 (1989).

15. J.B. Cross, S.L. Koontz, and J.C. Gregory, "Laboratory Investigations Involving High-Velocity Oxygen Atoms", Proceedings of the Advanced Aerospace Materials Symposium, 119th TMS Annual Meeting and Exhibit, TMS, Warrendale, PA, Feb. 1990.
16. N.J. Chou, J. Parazczsak, E. Babich, Y.S. Chaug, and R. Goldblatt, Microelectron. Eng. 5, 375, (1986).
17. S.L.Koontz, Keith Albyn, and L.J. Leger, "Atomic Oxygen Testing with Thermal Atom Systems: A Critical Evaluation", J. Spacecraft and Rockets, 28, pp.315, 1991.
18. J.B. Cross, J.A. Martin, and L.E. Pope, in L.E. Pope, L.L. Fehrenbacher, and W.O. Winer (eds.) New Materials Approaches to Tribology: Therory and Applications, Vol. 140, Materials Research Society, Pittsburg, Pennsylvainia, 1989, pp. 271-276.
19 J. B. Cross, J.A. Martin, L.E. Pope, and S.L. Koontz,"Atomic Oxygen-MoS_2 Chemical Interactions", Surface and Coating Technology, 42, 41-48(1990).

END

DATE
FILMED
10128191